Effective temperature in fluctuation-driven Turing patterns*

Jinghui Liu
Department of Physics, Massachusetts Institute of Technology
77 Massachusetts Ave, Cambridge, MA 02139, USA
(Dated: May 18, 2018)

Application of effective temperature to evaluate non-equilibrium systems has been a motivated attempt to make connection with statistical thermodynamics, and has received small range success in systems like glass and colloids. On the other hand, its application in the broader class of quantitative biology models has been quite limited. Here we explore a Turing pattern model with noise-driven feature, and analytically evaluated the effective temperature for both species. We found an intriguing connection between effective temperature discrepancy and onset of the fluctuation-driven character in this particular system. The exploration could be encouraging for applying canonical thermodynamic quantity analysis in custom quantitative biology models.

PACS numbers: 05.40.Ca, 05.70.Ln

I. INTRODUCTION

Biological systems inherently operate out of equilibrium, while important statistical thermodynamics conclusion extend only till the near-equilibrium scenario. This separation of applicability poses significant difficulty when physicists work to understand biology systems. A handful of phenomenological models have been quantitatively developed and prove successful in describing network of molecules/species interacting, spatiotemporal organization of morphogens, etc., but few could be concluded taking advantage of fruits from existing statistical thermodynamics. Such contradiction then goes back to the long-standing debate whether there are physical quantities whose insights are extendible towards out-of-equilibrium systems.

The notion effective temperature was first employed as a way to test the breakdown of fluctuation-dissipation theorem (FDT) in systems far away from equilibrium, but various efforts were subsequently made to bridge this concept between equilibrium thermodynamics and more complex systems. Defined as the ratio of autocorrelation and response function, effective temperature is equal to the embedded heat bath temperature for a system at or near equilibrium, and differs if FDT breaks down. Attempts in evaluating effective temperature for out of equilibrium systems have been fruitful in certain cases. In glassy systems with peculiar aging dynamics, effective temperature was suggested to represent the heat bath temperature when the supercooled liquid first falls out of equilibrium[1]. This separation of time scales underlying this higher effective temperature is promisingly supported by simulation of sheared supercooled liquid[2]. In active colloidal systems, the defined effective temperature was experimentally shown to control the steady state phase separation behavior, and the phase transition process qualitatively represents its thermal equilibrated counterparts[4].

Application of effective temperature in custom quantitative biology systems has turned out to be less straightforward. A generic example is the evaluation of effective temperature in stochastic gene networks/interacting species[5]. Depending on different perturbations done to the system, effective temperature defined with correlation and response function is no longer a unique quantity but observable-dependent, only converging in the large number limit when noise is negligible. These observations still make sense since we know steady states in those networks are never maintained at equilibrium; however, they bring less physics intuition other than emphasizing such out-of-equilibrium feature.

Despite those up and down sides of current effective temperature research, an intriguing while still unexamined application is towards spatially-extended pattern forming system. In this course paper, a specific Turing pattern system incorporating plankton-herbivore dynamics (Levin-Segel model, [7]), will be discussed. Selection of this particular model is based on two-fold concerns. Firstly, Fourier modes analysis of Turing patterns remains mathematically tractable even with intrinsic noise terms. Secondly, analysis of Levin-Segel model presents a regime of quasi-pattern[6], where parameters are still under Turing instability threshold but intrinsic noise spectrum selects for a particular wavelength. Exploration of effective temperature across differing pattern regimes might reveal hidden out-of-equilibrium physics.

Our goals are as following. First we aim to derive the analytic form of effective temperature, defined by the ratio of autocorrelation and response function when a particular Fourier mode is perturbed near steady state. We then compare the effective temperature across homogenous steady state, quasi-pattern regime, and near the onset of Turing instability. We also take advantage of the pre-calculated intrinsic noise structure of Levin-Segel model[6] in the first part.

* Coursework paper for 2017-2018 Spring 8.592J "Statistical Physics in Biology", taught by Prof. Kardar and Prof. Mirny

II. TURING PATTERNS IN LEVIN-SEGEL MODEL

As in common Turing pattern system, Levin-Segel Model is composed of two morphogens: an activator, A, and an inhibitor, B. A and B could also be considered as prey and predators if the model is applied to ecology system. A nonlinear growth term eA^2 in A are plugged in as predator satiation or prey Allen effect, and nonlinear degradation term $-dB^2$ in B represents competition. p is the parameter noting interaction (in this case B preys on/inhibits A) between the two species. With diffusivity represented by μ and ν for each species, the full equation set is as following

$$\begin{aligned}\frac{\partial A(x,t)}{\partial t} &= \mu\nabla^2 A + bA + eA^2 - pAB \\ \frac{\partial B(x,t)}{\partial t} &= \nu\nabla^2 B + pAB - dB^2\end{aligned} \tag{1}$$

Stability analysis reveals the model has a stable homogenous coexistence state, when $p > e$ and $p^2 > de$. The fixed point is at:

$$A_s = \frac{bd}{p^2 - de}, B_s = \frac{bp}{p^2 - de} \tag{2}$$

Like for typical Turing pattern system, expansion around this fixed point would give stability of the spatially homogenous state against small perturbations. An expansion and then Fourier transform from (x,t) to (k,t) space would give the following equations governing evolution of a particular Fourier mode k

$$\begin{aligned}A(x,t) &= A_s + \int dk e^{ikx}\tilde{A}(k,t) \\ B(x,t) &= B_s + \int dk e^{ikx}\tilde{B}(k,t)\end{aligned} \tag{3}$$

$$\frac{\partial}{\partial t}\begin{bmatrix}\tilde{A}\\ \tilde{B}\end{bmatrix} = M(k)\begin{bmatrix}\tilde{A}\\ \tilde{B}\end{bmatrix} \tag{4}$$

where $M(k)$ is the Jacobian around the fixed point for a particular wave number k:

$$M(k) = \begin{bmatrix} b + 2eA_s - pB_s - \mu k^2 & -pA_s \\ pB_s & pA_s - 2dB_s - \nu k^2\end{bmatrix} \tag{5}$$

and could be simplified to

$$M(k) = \begin{bmatrix} \frac{bde}{p^2-de} - \mu k^2 & \frac{bdp}{p^2-de} \\ -\frac{bp^2}{p^2-de} & -\frac{bdp}{p^2-de} - \nu k^2\end{bmatrix} \tag{6}$$

There is a Turing instability onset when maximum of eigenvalue for $M(k)$ exceeds zero. Straight-forward calculation could recover this criteria as a restriction on diffusivity ratio between the two species

$$\frac{\nu}{\mu} > \left(\frac{1}{(\sqrt{p/d} - \sqrt{p/d - e/p})}\right)^2 \tag{7}$$

And the wave number that has the maximum eigenvalue is

$$k_m = \sqrt{\frac{-\mu\frac{bp^2}{p^2-de} + \nu\frac{bde}{p^2-de}}{2\mu\nu}} = \sqrt{\frac{b}{2(p^2-de)}(-\frac{p^2}{\nu} + \frac{de}{\mu})} \tag{8}$$

From [6], intrinsic noise for a particular Fourier mode k of the system has the correlation matrix as

$$\begin{bmatrix}\mu Ak^2 + pAB + bAB + bA + eA^2 & -pAB \\ -pAB & \nu Bk^2 + pAB + dB^2\end{bmatrix} \tag{9}$$

It has been shown that even below Turing instability threshold (when v/u is not larger than criteria Turing instability equation), still there is a possibility of the noise spectrum giving a maximum at some nonzero k value, representing a fluctuation driven quasi Turing pattern. Calculation from [6] gives criteria for that nonzero k value to exist

$$\frac{\nu}{\mu} > \frac{p^3(5p^2 + 7de)}{e(4p^4 + 5p^2de + 3d^2e^2)} \tag{10}$$

This is essentially a relaxation of the diffusivity ratio requirement from tranditional Turing pattern. For a set of generic parameters $b = \frac{1}{2}$, $p = 1$, $d = \frac{1}{2}$ and $e = \frac{1}{2}$, equation (7) requires $\nu/\mu > 27.8$ while equation (10) relaxes it to $\nu/\mu > 2.48$.

Interestingly, under the noise-driven condition, the selected k value is the same as if real Turing pattern onsets: the k with maximum eigenvalue of $M(k)$. Thus the selected wave number is also

$$k_M = \sqrt{\frac{b}{2(p^2-de)}(-\frac{p^2}{\nu} + \frac{de}{\mu})} \tag{11}$$

as in equation (8).

The full phase diagram displaying spatially homogenous case, quasi-pattern case (fluctuation-driven Turing pattern) and Turing pattern case is as Fig 1.[6]. Intrinsic noise expanded the parameter regime where a particular wave number instability onsets.

III. EFFECTIVE TEMPERATURE CALCULATION

For a given wave number, Fourier transform from (x,t) to (k,t) space gives equation (3). Continuing to Fourier transform from (k,t) to (k,w) space gives the equation

$$\begin{aligned}-i\omega\hat{A} &= (-\mu k^2 + \frac{bde}{p^2-de})\hat{A} - \frac{bdp}{p^2-de}\hat{B} \\ -i\omega\hat{B} &= -\frac{bp^2}{p^2-de}\hat{A} + (-\nu k^2 - \frac{bdp}{p^2-de})\hat{B}\end{aligned} \tag{12}$$

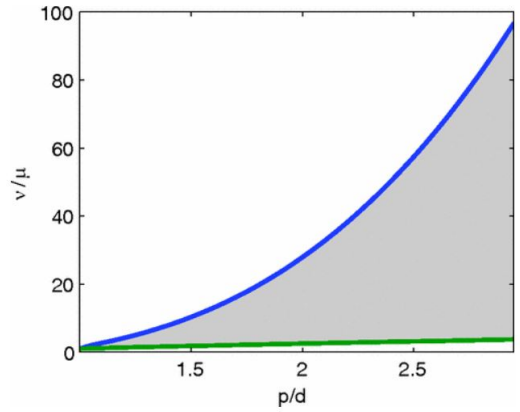

FIG. 1. Phase diagram of diffusivity ratio ν/μ: Blue line borders Turing instability regime (upper) and fluctuation-driven Turing regime (lower), while green line separates between fluctuation-driven Turing regime (upper) from spatially homogenous regime (lower). Plot is from [6]

.

where $\hat{A}$ and $\hat{B}$ come from

$$\tilde{A}(k,t) = \int d\omega e^{-i\omega t}\hat{A}(k,\omega)$$
$$\tilde{B}(x,t) = \int d\omega e^{-i\omega t}\hat{B}(k,\omega)$$

Adding noise term from interaction, taking advantage of intrinsic noise structure equation *, we get two linear equations for A(k,w) and B(k,w)

$$\begin{aligned} -i\omega\hat{A} &= (-\mu k^2 + \frac{bde}{p^2-de})\tilde{A} - \frac{bdp}{p^2-de}\hat{B} + D_1\hat{\xi_1} + D_3^a\hat{\xi_3} \\ -i\omega\hat{B} &= -\frac{bp^2}{p^2-de}\hat{A} + (-\nu k^2 - \frac{bdp}{p^2-de})\hat{B} + D_2\hat{\xi_2} + D_3^b\hat{\xi_3} \end{aligned} \tag{13}$$

where magnitude of the noise terms D_1, D_2 and D_3^a, D_3^b should satisfy the correlation matrix from equation (9). ξ_1, ξ_2 and ξ_3 represent normalized independent Gaussian white noise.

$$\begin{aligned} D_1 &= \sqrt{\mu k^2 A_s + pA_sB_s + bA_sB_s + bA_s + eA_s^2} \\ D_2 &= \sqrt{\nu k^2 B_s + pA_sB_s + dB_s^2} \\ D_3^a &= -\sqrt{p}B_s = -\frac{bp\sqrt{p}}{p^2-de} \\ D_3^b &= \sqrt{p}A_s = \frac{bd\sqrt{p}}{p^2-de} \end{aligned} \tag{14}$$

We could solve this equation to recover $A(k,\omega)$ and $B(k,\omega)$ as

$$\hat{A}(k,\omega) = \frac{D_1(\nu k^2 + \frac{bdp}{p^2-de})\hat{\xi}_1 - D_2\frac{bdp}{p^2-de}\hat{\xi}_2 + D_3^a(\nu k^2 + \frac{bdp}{p^2-de})\hat{\xi}_3 - D_3^b\frac{bdp}{p^2-de}\hat{\xi}_3 - i\omega(D_1\xi_1 + D_3^a\xi_3)}{(\mu k^2 - \frac{bde}{p^2-de})(\nu k^2 + \frac{bdp}{p^2-de}) - \omega^2 + \frac{b^2p^3d}{(p^2-de)^2} - i\omega((\mu k^2 - \frac{bde}{p^2-de}) + (\nu k^2 + \frac{bdp}{p^2-de}))} \tag{15}$$

$$\hat{B}(k,\omega) = \frac{D_1(\frac{bp^2}{p^2-de})\hat{\xi}_1 + D_2(\mu k^2 - \frac{bde}{p^2-de})\hat{\xi}_2 + D_3^a\frac{bp^2}{p^2-de}\hat{\xi}_3 + D_3^b(\mu k^2 - \frac{bde}{p^2-de})\hat{\xi}_3 - i\omega(D_2\xi_2 + D_3^b\xi_3)}{(\mu k^2 - \frac{bde}{p^2-de})(\nu k^2 + \frac{bdp}{p^2-de}) - \omega^2 + \frac{b^2p^3d}{(p^2-de)^2} - i\omega((\mu k^2 - \frac{bde}{p^2-de}) + (\nu k^2 + \frac{bdp}{p^2-de}))} \tag{16}$$

The real part of autocorrelation function could be recovered under careful calculation and a series of simplifications,

$$C'_{AA} = \frac{D_1^2(\nu k^2 + \frac{bdp}{p^2-de})^2 + D_2^2(\frac{bdp}{p^2-de})^2 + (D_3^a(\nu k^2 + \frac{bdp}{p^2-de}) - D_3^b\frac{bdp}{p^2-de})^2 + \omega^2(D_1^2 + D_3^{a2})}{((\mu k^2 - \frac{bde}{p^2-de})(\nu k^2 + \frac{bdp}{p^2-de}) - \omega^2 + \frac{b^2p^3d}{(p^2-de)^2})^2 + \omega^2((\mu k^2 - \frac{bde}{p^2-de}) + (\nu k^2 + \frac{bdp}{p^2-de}))^2} \tag{17}$$

$$C'_{BB} = \frac{D_1^2(\frac{bp^2}{p^2-de})^2 + D_2^2(\mu k^2 - \frac{bde}{p^2-de})^2 + (D_3^a\frac{bp^2}{p^2-de} + D_3^b(\mu k^2 - \frac{bde}{p^2-de}))^2 + \omega^2(D_2^2 + D_3^{b2})^2}{((\mu k^2 - \frac{bde}{p^2-de})(\nu k^2 + \frac{bdp}{p^2-de}) - \omega^2 + \frac{b^2p^3d}{(p^2-de)^2})^2 + \omega^2((\mu k^2 - \frac{bde}{p^2-de}) + (\nu k^2 + \frac{bdp}{p^2-de}))^2} \tag{18}$$

Likewise, response function of the system could be calculated assuming we perturb equation set (13) with terms

$\hat{h_1}(w)$ and $\hat{h_2}(w)$

$$\begin{aligned} -i\omega\hat{A} &= (-\mu k^2 + \frac{bde}{p^2-de})\tilde{A} - \frac{bdp}{p^2-de}\hat{B} + D_1\hat{\xi_1} + D_3^a\hat{\xi_3} + \hat{h_1}(w) \\ -i\omega\hat{B} &= -\frac{bp^2}{p^2-de}\hat{A} + (-\nu k^2 - \frac{bdp}{p^2-de})\hat{B} + D_2\hat{\xi_2} + D_3^b\hat{\xi_3} + \hat{h_2}(w) \end{aligned} \tag{19}$$

And the imaginary part of responses of $\hat{A}$ and $\hat{B}$ could be determined as

$$R_{AA}^{''} = (\frac{\delta\langle\hat{A(\omega)}\rangle}{\delta\hat{h_1}(\omega)})^{''} = \frac{\omega(\omega^2 - (\mu k^2 - \frac{bde}{p^2-de})(\nu k^2 + \frac{bdp}{p^2-de}) - \frac{b^2p^3d}{(p^2-de)^2} + (\nu k^2 + \frac{bdp}{p^2-de})((\mu+\nu)k^2 + \frac{bd(p-e)}{p^2-de}))}{((\mu k^2 - \frac{bde}{p^2-de})(\nu k^2 + \frac{bdp}{p^2-de}) - \omega^2 + \frac{b^2p^3d}{(p^2-de)^2})^2 + \omega^2((\mu k^2 - \frac{bde}{p^2-de}) + (\nu k^2 + \frac{bdp}{p^2-de}))^2} \tag{20}$$

$$R_{BB}^{''} = (\frac{\delta\langle\hat{B(\omega)}\rangle}{\delta\hat{h_2}(\omega)})^{''} = \frac{\omega(\omega^2 - (\mu k^2 - \frac{bde}{p^2-de})(\nu k^2 + \frac{bdp}{p^2-de}) - \frac{b^2p^3d}{(p^2-de)^2} - (\mu k^2 - \frac{bde}{p^2-de})((\mu+\nu)k^2 + \frac{bd(p-e)}{p^2-de}))}{((\mu k^2 - \frac{bde}{p^2-de})(\nu k^2 + \frac{bdp}{p^2-de}) - \omega^2 + \frac{b^2p^3d}{(p^2-de)^2})^2 + \omega^2((\mu k^2 - \frac{bde}{p^2-de}) + (\nu k^2 + \frac{bdp}{p^2-de}))^2} \tag{21}$$

Combining those together, what we get is an expression for effective temperature based on evaluating autocorrelation and response function of species A and B

$$T_{eff}^{AA} = \frac{\omega C_{AA}^{'}(k,\omega)}{R_{AA}^{''}(k,\omega)} = \frac{D_1^2(\nu k^2 + \frac{bdp}{p^2-de})^2 + D_2^2(\frac{bdp}{p^2-de})^2 + (D_3^a(\nu k^2 + \frac{bdp}{p^2-de}) - D_3^b\frac{bdp}{p^2-de})^2 + \omega^2(D_1^2 + D_3^{a2})}{\omega^2 - (\mu k^2 - \frac{bde}{p^2-de})(\nu k^2 + \frac{bdp}{p^2-de}) - \frac{b^2p^3d}{(p^2-de)^2} + (\nu k^2 + \frac{bdp}{p^2-de})((\mu+\nu)k^2 + \frac{bd(p-e)}{p^2-de})} \tag{22}$$

$$T_{eff}^{BB} = \frac{\omega C_{BB}^{'}(k,\omega)}{R_{BB}^{''}(k,\omega)} = \frac{D_1^2(\frac{bp^2}{p^2-de})^2 + D_2^2(\mu k^2 - \frac{bde}{p^2-de})^2 + (D_3^a\frac{bp^2}{p^2-de} + D_3^b(\mu k^2 - \frac{bde}{p^2-de}))^2 + \omega^2(D_2^2 + D_3^{b2})^2}{\omega^2 - (\mu k^2 - \frac{bde}{p^2-de})(\nu k^2 + \frac{bdp}{p^2-de}) - \frac{b^2p^3d}{(p^2-de)^2} - (\mu k^2 - \frac{bde}{p^2-de})((\mu+\nu)k^2 + \frac{bd(p-e)}{p^2-de})} \tag{23}$$

Notice that if we tune p to 0 (though it'll be an unphysical situation since then species A would not have fixed point), equation (22) and equation (23) would essentially reduce to $T_{eff}^{AA} = D_1^2$ and $T_{eff}^{BB} = D_2^2$. This simple reasoning makes a lot sense, since when interaction between species is tuned to zero, we'll expect effective temperature of both species only depending on their internal dynamics.

With this expression we can then pull in expression of D_1, D_2, D_3^a and D_3^b from equation (14) to get rid of most parameters except for k and ω.

A. ω dependence

Recall that Turing and fluctuation-driven Turing pattern select for the same wave number as equation (8), the expression of T_{eff}^{AA} and T_{eff}^{BB} could be simplified to $T_{eff}^{AA}(\omega)$ and $T_{eff}^{BB}(\omega)$ when we're only interested in the system's behavior at the particular k_M.

To qualitatively see the dependence of effective temperature on ω, we fix other irrelevant parameters (p,d,e) at a generic parameter set $b = \frac{1}{2}$, $p = 1$, $d = \frac{1}{2}$ and $e = \frac{1}{2}$. Then border between Turing instability and fluctuation driven instability is at $\nu/\mu > 27.8$ (equation (7)), while border between fluctuation driven instability and spatial homogenity is at $\nu/\mu > 2.48$ (equation (10)). For easier comparison, we set $\mu = 1$ and vary ν to cross those two borders and plot for the effective temperature for A and B.

Figure 2 shows the effective temperature over frequency plot for four sets of diffusivity ratio: $\nu/\mu = 1$, $\nu/\mu = 2.5$, $\nu/\mu = 10$ and $\nu/\mu = 27$. As we could see, near the onset of fluctuation-driven instability, discontinuity position for species A and B coincide; such collision does not persist when diffusivity ratio is further

increased. Near onset of Turing instability, both species lose the discontinuity in $T_{eff} - \omega$ and display a smooth temperature difference change across a wide change of ω, again emphasizing the non-equilibrium nature of the system.

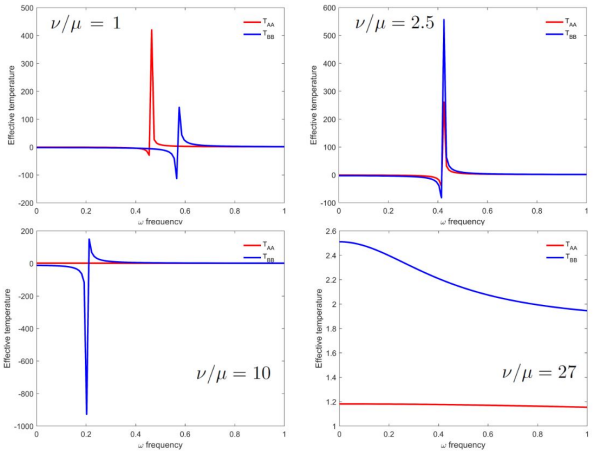

FIG. 2. Effective temperature versus frequency plot varying ν/μ: Blue line represents species B while red line represents species A. Discontinuity position of both species collide near onset of fluctuation-driven instability. Here $k = k_M$, selecting the wave number with largest eigenvalue for visualization.

B. k dependence

A similar analysis that should be doable is dependence of effective temperature on wave number k, when frequency ω is fixed or at the discontinuity point. Limited by time and energy this analysis has not been performed; However, based on what we know for onsets of both instabilities– that the pattern always selects for the wave number with largest eigenvalue– there is reason to believe what is physically meaningful has been done in the previous part, when we fix the wave number to k_M.

IV. CONCLUSION

Over this project, we attempted the evaluation of effective temperature in a spatially extended system with intrinsic noise. For Levin-Segel model that's versatile in describing either activator-inhibitor morphogen dynamics or prey-predator ecology, intrinsic noise confers an additional type of instability, relaxing the diffusivity requirement for the onset of Turing instability. Based on the intrinsic noise structure formulated by [6], we did a series of analytic calculation and successfully recovered the effective temperature formula when specifying Fourier modes, and retrieved meaningful physics intuition from the results.

There are several interesting features from our results plot in Fig 2. First, in a spatial homogeneous parameter regime, effective temperature of both species are equal and zero except for a discrepancy point near some critical ω. Secondly, such discrepancy points for the two species do not collide until onset of fluctuation-driven instability, reported by [6]. When approaching Turing instability onset point, discrepancy along frequency curve disappear one after the other, and the effective temperature starts to run around a finite value– and of course, are different for both species, in agreement with non-equilibrium nature of pattern-forming systems.

The analysis we have done is still coarse in many ways. For example, we're only considering perturbation near the fixed point that represents a spatially homogeneous system. Strictly speaking, for diffusivity ratio satisfying Turing pattern criteria, after the most significant wave number took over, analysis of Fourier mode near the homogenous state won't be informative anymore. However, (mostly for the author) it is still intriguing to see certain footprints are conserved even in the language of effective temperature, which is a seldom visited idea in field of spatiotemporal pattern organization.

[1] Kurchan, J. (2005). In and out of equilibrium. Nature, 433(7023), pp.222-225.

[2] Berthier, L. and Barrat, J. (2002). Nonequilibrium dynamics and fluctuation-dissipation relation in a sheared fluid. The Journal of Chemical Physics, 116(14), pp.6228-6242.

[3] Wang, S. and Wolynes, P. (2011). Communication: Effective temperature and glassy dynamics of active matter. The Journal of Chemical Physics, 135(5), p.051101.

[4] Han, M., Yan, J., Granick, S. and Luijten, E. (2017). Effective temperature concept evaluated in an active colloid mixture. Proceedings of the National Academy of Sciences, 114(29), pp.7513-7518.

[5] Lu, T., Hasty, J. and Wolynes, P. (2006). Effective Temperature in Stochastic Kinetics and Gene Networks. Biophysical Journal, 91(1), pp.84-94.

[6] Butler, T. and Goldenfeld, N. (2011). Fluctuation-driven Turing patterns. Physical Review E, 84(1).

[7] LEVIN, S. and SEGEL, L. (1976). Hypothesis for origin of planktonic patchiness. Nature, 259(5545), pp.659-659.